Observation of Topological Uhlmann Phase in Superconducting Qubits

Kelton Madden
Department of Physics and Astronomy
University of Pennsylvania
May 4, 2020

The topological Uhlmann phase characterizes mixed state systems unable to be described using the standard Berry phase. We show measurement of this observable in a topological insulator simulated through entangled superconducting qubits using *IBM's Quantum Experience*. The complete topological phase and environmental information of both state-dependant and and state-independent mixed states, normally inaccessible, are shown to be extracted through use of ancilla states. The procedures outlined are extendable to more complex topological and interacting systems with a large number of energy bands.

I. Introduction

Topological phase has become a subject of great theoretical and experimental interest in its application to recent breakthroughs in condensed matter physics (eg. the TKNN invariant characterization of Hall conductance [1]). The notions of Berry phase and Berry curvature are intrinsically related to the topological invariants of such systems, and have been crucial in understanding the properties of topological insulators (TIs) superconductors (TSCs), quantum hall states, and other topological phenomena [2–4]. These topological systems are important to study for the continued development of a modern understanding of condensed matter systems and their ability to form the basis of novel quantum computing architectures [5–7]. Berry phase, and other topological phase classifications, are strictly geometric and therefore independent of dynamical phase contributions and path disturbance throughout the evolution of a given quantum state. The topological character of such geometric phase, combined with the exotic band structure of TIs, TSCs, and other condensed matter systems, are what enable the non-local encoding of quantum information which has potential for use in scalable quantum computing [7].

Berry phase as an observable quantity, however, is only applicable to pure state systems unaffected by environmental noise, a rare condition for TIs and TSCs where, for example, thermal fluctuations are almost guaranteed to be present. The first solution to model topological phase for mixed states was proposed by Uhlmann in 1986 and soon followed by further theoretical development on his part [8, 9]. His original elucidation was quite mathematically rigorous, however, the formulation remains an elegant and natural extension of the gauge invariant Berry phase. Recently, Uhlmann phase has been applied to 1D and 2D dimensional exotic condensed matter systems (eg: Majorana Chains, 2D TSCs, Haldane Model) [10–12], however, it was only in 2018, that Viyuela, et al. experimentally measured this phase using superconducting qubits [13]. In this work we emulate this achievement.

Our results demonstrate the measurement of the Uhmann phase, simulated using superconducting qubits, for a range of mixed states. We display the phase diagram for when the initial mixed state is known (state dependent) as well as when the initial state is unknown (state independent). Both cases reveal a clear transition of the topological phase from π to 0 as the mixedness of the state increases, which can be physically interpreted as the exceeding of a critical temperature or environmental noise limit. Our results display simulation of the AIII TIs class, specifically those with chiral symmetry, in the presence of external noise. The protocol used can be translated for measuring topological phase (of mixed states) of 2D TIs, TSCs, and interacting systems with proper modification.

II. Theoretical Proof of Concept

The Uhlmann phase is defined such that the mixed state becomes a subspace of an enlarged pure state using standard purification techniques. The U(n)-gauge freedom (n being the dimension of the Hilbert Space) of the Uhlmann phase can be seen as a generalization of the U(1) freedom of the Berry phase in which $|\psi\rangle$ and $e^{i\phi}|\psi\rangle$ represent the same physical state (see Figure 1). This freedom comes from defining the construction of an arbitrary density

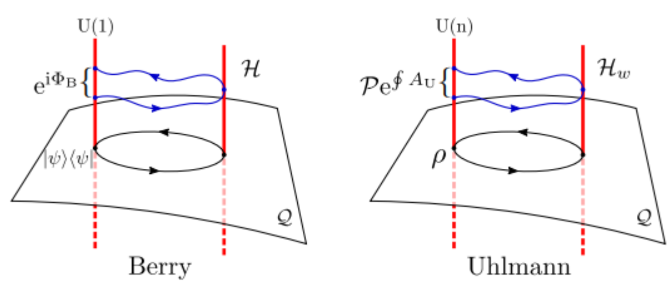

FIG. 1. Comparison between Berry and Uhlmann Holonomies. In the Berry approach, valid for pure states, after a closed loop on the space $\mathcal{Q}$, the final state accumulates a phase Φ_B with respect to the initial state vector. In the Uhlmann approach, formulated for mixed states, the initial and final state differ by a unitary matrix given by $\mathcal{P}e^{\oint A}$. Figure from Viyuela, et al., 2014 [10].

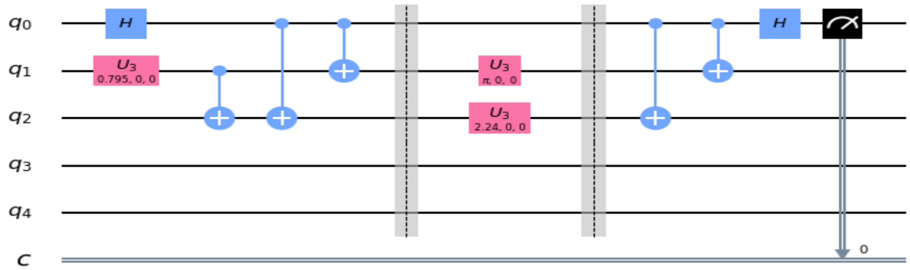

FIG. 2. Circuit diagram from *IBM Quantum Experience* for the measurement of the topological Uhlmann Phase, specifically $\langle\sigma_x\rangle$, for the mixed state r = .15. All rotations are around the y axis, with the first R_y on q[1] = $2arccos(\sqrt{1-r}) = 0.7954$, the second R_y on q[1] = π, and the third R_y on q[2] = $2\pi\sqrt{r(1-r)}$.

matrix ρ using amplitudes w which form a Hilbert space $\mathcal{H}_w$ such that

$$\rho = ww^\dagger, \tag{1}$$

with the Hibert-Schmidt product $\langle w_1^\dagger, w_2\rangle = Tr(w_1^\dagger w_2)$.

The U(n) gauge-freedom is result of the fact that by definition w and wU are amplitudes of the same state. By the polar decomposition theorem, the amplitudes of some density matrix ρ are parametrized as $\sqrt{w}U$ and $\rho = \sum_j p_j |\psi_j\rangle\langle\psi_j|$ with $w = \sum_j \sqrt{p_j}|\psi_j\rangle\langle\psi_j|\, U$, from the spectral theorem. The purification works using the following isomorphism between the aforementioned space $\mathcal{H}_w$ and $\mathcal{H}\otimes\mathcal{H}$: $w = \sum_j \sqrt{p_j}|\psi_j\rangle\langle\psi_j|\, U \leftrightarrow |w\rangle = \sum_j \sqrt{p_j}|\psi_j\rangle \otimes U^t|\psi_j\rangle$. The density matrix $\rho = ww^\dagger$ in the purification space can be traced out as

$$\rho = Tr_2(|w\rangle\langle w|). \tag{2}$$

Tr_2 represents the partial trace over the second Hilbert space of $\mathcal{H}\otimes\mathcal{H}$, from which it is clear the unitary (U) component of the amplitude is arbitrary. It is evident that any amplitude w of some density matrix ρ can be transformed to a pure state $|w\rangle$ of an enlarged space with the partial trace equal to ρ. As seen in Fig. 1, the Berry phase of some state $|\psi\rangle$ after completing a closed trajectory on some space $\mathcal{Q}$ can be written $e^{i\Phi_B}|\psi\rangle$ with $\Phi_B = \oint A_B$ and $A_B := i\sum_\mu \langle\psi_k|\partial/\partial k_\mu \psi_k\rangle\, dk_\mu$ defined as the Berry connection form. Analogous to the pure state transformation, Uhlmann defines a parallel transport condition such that after the state completes a closed path, the initial and final amplitudes differ by some unitary transformation V, such that $w_{(0)} = w_{(T)}V$. The parallel transport is satisfied with $V := \mathcal{P}e^{\oint A_U}U_0$; where $\mathcal{P}$ is the path ordering operator (which is in the 1D TI case is abelian and therefore trivial), A_U the Uhlmann connection, and U_0 the gauge from t = 0. The parallel transport condition requires that V is constructed so that the distance between two infinitesimally close purifications, $\||\psi_{(t+dt)}\rangle - |\psi_{(t)}\rangle\|^2$, reaches its minimum value, satisfied with V as defined above. With this satisfied, an explicit formula of A_U, in the spectral basis of $\rho_\theta = \sum_j p_\theta^j |\psi_\theta^j\rangle\langle\psi_\theta^j|$, (note: we are still indexing over j, but have introduced θ as a parameter of path taken; θ maps the crystalline momentum in condensed matter systems), is given by Hübner [14] as:

$$A_U = \sum_{i,j} |\psi_\theta^i\rangle \frac{\langle\psi_\theta^i|\,[(\partial_\theta\sqrt{\rho_\theta}), \sqrt{\rho_\theta}]\,|\psi_\theta^j\rangle}{p_\theta^i + p_\theta^j}\langle\psi_\theta^j|\, d\theta, \tag{3}$$

with $\theta(t)|_{t=0}^T$ defining a trajectory along possible single qubit density matrices parametrized by θ. The density matrix of the two-band TI of the AIII chiral-unity class [15] is defined

$$\rho_\theta = (1-r)\,|0_\theta\rangle\langle 0_\theta| + r\,|1_\theta\rangle\langle 1_\theta|, \tag{4}$$

$$|0_\theta\rangle = \frac{1}{\sqrt{1+g^2(\theta,M)}}(1, g(\theta,M))^T, \tag{5}$$

$$|1_\theta\rangle = \frac{1}{\sqrt{1+g^2(\theta,M)}}(g(\theta,M), -1)^T, \tag{6}$$

where r is the degree of mixedness between ground and excited state and M is the hopping amplitude for which the system is only topological with M < 1. Simplifying (3) using (4) gives,

$$A_U = [(1-p_r)\langle 1_\theta|\partial_\theta 0_\theta\rangle\,|0_\theta\rangle\langle 1_\theta| + (1-p_r)\langle 0_\theta|\partial_\theta 1_\theta\rangle\,|0_\theta\rangle\langle 1_\theta|]d\theta, \tag{7}$$

where $p_r = 2\sqrt{r(1-r)}$. The differential inner products correspond to the winding vector and the simplified equation for the Uhlmann connection yields,

$$A_U(\theta) = -i(1-p_r)\frac{\partial_\theta n_\theta^x}{2n_\theta^z}\sigma_y d\theta, \tag{8}$$

where $n_\theta^i$is the ith component of the winding vector. Plugging (6) into into the Uhlmann unitary V_A and computing the Uhlmann phase with M < 1 and critical topological transition temperatures of $r_{c1} = \frac{1}{4}(2-\sqrt{3}) \approx 0.067$ and $r_{c2} = 1 - r_{c1} \approx .93$, results in

$$\Phi_U = arg[\langle\Psi_{\theta=0}|\Psi_{\theta=T}\rangle] = argTr[\rho_{\theta(0)}V_A] = arg\left\{-cos(2\pi\sqrt{r(1-r)})\right\}. \tag{9}$$

III. Experimental Measurement

Measurement of the Uhlmann phase is a challenging problem, as a requirement of the purification is precise

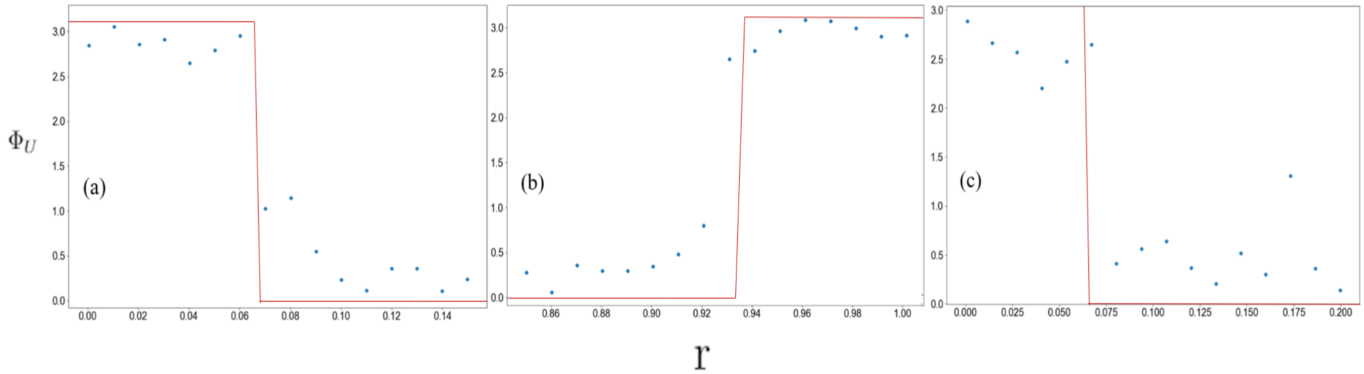

FIG. 3. In all figures the mixedness parameter (r) vs. Uhlmann phase (Φ_U) is displayed with the red function indication the theoretical value of the topological phase. (a) displays the results for the state dependent protocol at r_{c1}, (b) displays the results for the state dependent protocol at r_{c2}, (c) displays results for the state independent protocol at r_{c1} for a larger range of r.

control of the environmental (or ancilla) degrees of freedom. To measure the phase in our superconducting qubit simulation we use an ancilla qubit (q2), representing the environment, and a probe qubit (q0) to extract the phase using standard interferometric techniques. The circuit design as displayed in IBMS's *Qiskit* is shown in Fig. 2.

Initialization: The mixedness parameter of the state is initialized with a R_y rotation $2arccos(\sqrt{1-r})$ and a controlled not gate, resulting in the state $|\psi_{\theta(0)}\rangle \otimes |0_\theta\rangle$.

Adiabatic Unitary Transport: Next, we entangle the probe qubit with the system and ancilla qubits using two sets of controlled not operations, from probe to ancilla and system, with intermediary R_y rotations of the system and ancilla by β_1, β_2 respectively. The values of β_1 and β_2 are determined by A_U and p_a. To satisfy the parallel transport condition, in the state-dependent protocol, $\beta_1 = \pi$ and $\beta_2 = p_a\beta_1$ with $p_a = p_r$. In the state-independent protocol, $\beta_1 = \int_t A_U$, for a non-trivial path parameter t, and β_2 = -arctan($\frac{2}{tan\beta_1}$), with M, t = .6 [13].

Trace out/Read out: After the holonomic evolution, the qubits S, A, P are in the superposition state

$$|\Psi_{SAP}\rangle = \frac{1}{\sqrt{2}}(|\psi_{\theta(0)}\rangle \otimes |0\rangle_P \; + \; |\psi_{\theta(T)}\rangle \otimes |1\rangle_P). \quad (10)$$

Tracing out the system and ancilla from (11) gives,

$$\rho_P = \frac{1}{2}(Re(\langle\psi_{\theta(0)}|\psi_{\theta(T)}\rangle\, \sigma_x) + Im(\langle\psi_{\theta(0)}|\psi_{\theta(T)}\rangle)\sigma_y). \quad (11)$$

Therefore, from the Probe qubit, we can measure Φ_U as

$$\Phi_U = arg\left\{\langle\sigma_x\rangle - i\,\langle\sigma_y\rangle\right\} \quad (12)$$

The experimental results of these measurements for the state dependent and independent protocols are shown in Fig. 3. The circuit was carried out using IBM's QASM controlling three transmon qubits coupled using co-planar waveguide resonators. We specifically used the imbq-rome quantum computer which was measured on the day of use to have relaxation and decoherence times: T1(q0, q1, q2) = ($71.1_{\mu s}, 97.4_{\mu s}, 73.6_{\mu s}$) and T2(q0, q1, q2) = ($66.9_{\mu s}, 57.8_{\mu s}, 89.3_{\mu s}$). The critical topological transitions at r_{c1} and r_{c2} are clearly visible regardless of state dependence/independence.

IV. Conclusion and Future Applications

The results displayed in Fig. 3 closely follow theoretical predictions for the Uhlmann phase as well as Viyuela, et al.'s results. Although there are deviations from the theoretical prediction, evident near critical r values and in the state independent protocol's magnitude, these deviations can be explained though faulty initialization, gate errors, spontaneous emission, relaxation times, and dephasing. Even with experimental error, the topological transition is clearly seen for all three graphs displayed in Fig. 3. Compared with the Viyuela, et al. group, our measurements are consistently similar, however, theirs display a flatter trend away from the critical values. An explanation for this difference is their introduction of an offset term in the case of the state independent protocol [13], and use of tighter error metrics derived from IBMQ error quantities. These corrections and dynamic decoupling techniques could all be incorporated in successive experiments for greater accuracy. The results used standard binomial distribution error for error bars which ended up so small they are not visible, however, Viyuela's results show an increase in error in the state independent result in their use of a different error metric. In general, let it be noted this simulation assumes one ancilla properly encodes the mixedness of a state and environment.

Looking forward, similar experimental results can be derived for condensed matter systems with higher dimension, complex band structures, and interacting components using novel Berry and Uhlmann techniques [12, 16] that are inaccessible classically. This quantum exploration of condensed matter physics hearkens to NISQ era use of quantum computers to realize Feynman's original computational dream of using quantum systems to further our knowledge of matter itself.

[1] D. J. Thouless, M. Kohmoto, M. P. Nightingale, and M. den Nijs, Quantized hall conductance in a two-dimensional periodic potential, Physical review letters **49**, 405 (1982).
[2] B. A. Bernevig, T. L. Hughes, and S.-C. Zhang, Quantum spin hall effect and topological phase transition in hgte quantum wells, Science **314**, 1757–1761 (2006).
[3] L. Fu and C. L. Kane, Topological insulators with inversion symmetry, Physical Review B **76**, 10.1103/physrevb.76.045302 (2007).
[4] M. Z. Hasan and C. L. Kane, Colloquium: Topological insulators, Reviews of Modern Physics **82**, 3045–3067 (2010).
[5] A. Kitaev, Fault-tolerant quantum computation by anyons, Annals of Physics **303**, 2–30 (2003).
[6] J. Pachos, P. Zanardi, and M. Rasetti, Non-abelian berry connections for quantum computation, Physical Review A **61**, 10.1103/physreva.61.010305 (1999).
[7] C. Nayak, S. H. Simon, A. Stern, M. Freedman, and S. Das Sarma, Non-abelian anyons and topological quantum computation, Reviews of Modern Physics **80**, 1083–1159 (2008).
[8] A. Uhlmann, Parallel transport and "quantum holonomy" along density operators, Reports on Mathematical Physics **24**, 229 (1986).
[9] A. Uhlmann, On berry phases along mixtures of states, Annalen der Physik **501**, 63 (1989).
[10] O. Viyuela, A. Rivas, and M. Martin-Delgado, Uhlmann phase as a topological measure for one-dimensional fermion systems, Physical Review Letters **112**, 10.1103/physrevlett.112.130401 (2014).
[11] O. Viyuela, A. Rivas, and M. A. Martin-Delgado, Symmetry-protected topological phases at finite temperature, 2D Materials **2**, 034006 (2015).
[12] O. Andersson, I. Bengtsson, M. Ericsson, and E. Sjöqvist, Geometric phases for mixed states of the kitaev chain, Philosophical Transactions of the Royal Society A: Mathematical, Physical and Engineering Sciences **374**, 20150231 (2016).
[13] O. Viyuela, A. Rivas, S. Gasparinetti, A. Wallraff, S. Filipp, and M. A. Martin-Delgado, Observation of topological uhlmann phases with superconducting qubits, npj Quantum Information **4**, 10.1038/s41534-017-0056-9 (2018).
[14] M. Hübner, Computation of uhlmann's parallel transport for density matrices and the bures metric on three-dimensional hilbert space, Physics Letters A **179**, 226 (1993).
[15] A. Kitaev, V. Lebedev, and M. Feigel'man, Periodic table for topological insulators and superconductors, AIP Conference Proceedings 10.1063/1.3149495 (2009).
[16] P. Roushan, C. Neill, Y. Chen, M. Kolodrubetz, C. Quintana, N. Leung, M. Fang, R. Barends, B. Campbell, Z. Chen, and et al., Observation of topological transitions in interacting quantum circuits, Nature **515**, 241–244 (2014).